

Phase transitions and dynamics of bulk and interfacial water

This article has been downloaded from IOPscience. Please scroll down to see the full text article.

2010 J. Phys.: Condens. Matter 22 284103

(<http://iopscience.iop.org/0953-8984/22/28/284103>)

View [the table of contents for this issue](#), or go to the [journal homepage](#) for more

Download details:

IP Address: 80.3.228.247

The article was downloaded on 22/06/2010 at 08:57

Please note that [terms and conditions apply](#).

Phase transitions and dynamics of bulk and interfacial water

G Franzese¹, A Hernando-Martínez¹, P Kumar², M G Mazza³,
K Stokely³, E G Strekalova³, F de los Santos⁴ and H E Stanley³

¹ Departament de Física Fonamental, Universitat de Barcelona, Diagonal 647,
Barcelona 08028, Spain

² Center for Studies in Physics and Biology, Rockefeller University, 1230 York Avenue,
New York, NY 10021, USA

³ Center for Polymer Studies and Department of Physics, Boston University, Boston,
MA 02215, USA

⁴ Departamento de Electromagnetismo y Física de la Materia, Universidad de Granada,
Fuentenueva s/n, 18071 Granada, Spain

E-mail: gfranzese@ub.edu

Received 8 December 2009, in final form 18 March 2010

Published 21 June 2010

Online at stacks.iop.org/JPhysCM/22/284103

Abstract

New experiments on water at the surface of proteins at very low temperature display intriguing dynamic behaviors. The extreme conditions of these experiments make it difficult to explore the wide range of thermodynamic state points needed to offer a suitable interpretation. Detailed simulations suffer from the same problem, where equilibration times at low temperature become extremely long. We show how Monte Carlo simulations and mean field calculations using a tractable model of water help interpret the experimental results. Here we summarize the results for bulk water and investigate the thermodynamic and dynamic properties of supercooled water at an interface.

1. Introduction

Water is essential in biology, because it participates in nearly every process necessary for life (including cell metabolism, transport of nutrients and residues, protein conformation changes, etc), and is the most common solvent in chemistry. It regulates a large variety of processes, including atmospheric phenomena, the formation of geophysical structures, the propagation of cracks in stones and cement, the sliding of glaciers, the transport in plants, and is ubiquitous in the universe as ice in the interstellar space. In all these examples the properties of water are essential to understand what is observed.

Nevertheless, water has proven to be a complex puzzle to many researchers for its anomalous thermodynamic and dynamic properties at room temperature and pressure. For example, by decreasing temperature T at pressure $P = 1$ atm, water's volume fluctuations, proportional to the isothermal compressibility K_T , increase below $T = 46^\circ\text{C}$, and entropy fluctuations, proportional to the isobaric specific heat C_P increase below $T = 35^\circ\text{C}$, while in a normal liquid any fluctuation decreases when T is decreased [1–3]. These water

anomalies grow upon cooling and increase in number. For example, below $T = 4^\circ\text{C}$ the cross-fluctuation of volume and entropy, proportional to the isobaric thermal expansion coefficient α_P , becomes negative [4], while it is always positive in normal liquids where the entropy decreases when the volume decreases [5].

By decreasing T even more, it is experimentally possible to supercool liquid water down to $T_H = -41^\circ\text{C}$ at 1 atm and to $T_H = -92^\circ\text{C}$ at 2000 atm, where the liquid is metastable with respect to crystal phases [1]. These extreme conditions are not unusual in nature, where water exists in its liquid form at -20°C in insects, -37°C in clouds or -47°C in plants [6]. Below T_H the homogeneous nucleation of crystalline ice occurs in a time too short to allow any measurements. But even the crystal phase of water is not simple. In fact, water is a polymorph with at least sixteen forms of crystal ices, the last one, Ice XV, was discovered in 2009 [7].

However, at very low T , crystal water is not the only possible kind of ice. By rapidly quenching liquid water below -123°C [8], or by condensing the vapor at low T [9], or by compressing crystal ice at low T [10], or by irradiation (with ions for example [11]), it is possible to solidify water

as an amorphous, or glass, i.e. a form that has the elastic properties of a solid, but the structure of a liquid with no long-range order [12]. As for the crystal state, the amorphous state of water is also not unique. Water is a polyamorph with at least three different amorphous states: low-density amorphous (LDA), discovered in 1935 [13], high-density amorphous (HDA), discovered in 1984 [14], and very high-density amorphous ice (VHDA), discovered in 2001 [15].

All these anomalies are a consequence of the properties of the hydrogen bond network that water forms. The hydrogen bond interaction is characterized by a preferred geometrical configuration, that at low T and P is approximately a tetrahedron of four molecules around a central one, with an angle varying around 106.6° (slightly smaller than a tetrahedral angle of 109.47°) and a distance oscillating around 2.82 \AA [5]. The local arrangement, including the number of nearest neighbors, can change with T and P . In particular, in 2000 Soper and Ricci observed at 268 K, compressing from 26 to 400 MPa, a continuous transformation from low-density liquid (LDL) local arrangement of water with an open, hydrogen-bonded tetrahedral structure, to high-density liquid (HDL) local arrangement with nontetrahedral O–O–O angles and a collapsed second coordination shell with broken hydrogen bonds, and a change in density of about 73% [16].

1.1. Thermodynamic interpretations of water behavior

All the above results are consistent with theories that propose different mechanisms and different phase behaviors in the supercooled region. They can be summarized in four possible scenarios for the P – T phase diagram.

(i) In the *stability limit* (SL) scenario [17] the behavior of the superheated liquid spinodal, i.e. the limit of stability of the liquid with respect to the gas, and the stretched water, i.e. water under tension as in a plant fibers, are related. In particular, it is hypothesized that the limits of stability of these two regions are continuously connected at negative pressure, forming a re-entrant curve toward the positive P region below $T_H(P)$. The response functions, including K_T , C_P and α_P , diverge when T is decreased at positive P as a consequence of the approaching of the re-entrant spinodal line.

(ii) In the *liquid–liquid critical point* (LLCP) scenario [18] it is hypothesized the existence of a LDL–HDL first-order phase transition line with negative slope in the P – T plane and terminating in a critical point C' . Below the critical pressure $P_{C'}$ the response functions increase on approaching the Widom line (the locus of correlation length maxima emanating from C' into the one-phase region) [5], and for $P > P_{C'}$ by approaching the HDL-to-LDL spinodal line. The possibility with $P_{C'} < 0$ have also been proposed [19].

(iii) In the *singularity-free* (SF) scenario [20] it is hypothesized that the low- T anticorrelation between volume and entropy gives rise to response functions that increase upon cooling and display maxima at non-zero T , but do not display any singular behavior. Specifically, Sastry *et al* [20] show that this is a direct consequence of the fact that water's line of temperatures of maximum density (TMD) has a negative slope in the (T, P) plane.

(iv) In the *critical point free* (CPF) scenario [21] it is hypothesized that a first-order phase transition line separates two liquid phases and extends to $P < 0$ toward the superheated limit of stability of liquid water. This scenario effectively predicts a continuous locus of stability limit spanning the superheated, stretched and supercooled state, because the spinodal associated with the first-order transition will intersect the liquid–gas spinodal at negative pressure. No critical point is present in this scenario.

Since all these scenarios are consistent with the available experimental data, a natural question is if we can design an experiment that would discriminate among them. Unfortunately, many scientists have discovered that finding an answer to this question is a difficult challenge [21]. In fact, experiments on bulk water are hampered by freezing below T_H , and no measurements on bulk liquid water can be performed with our present technology below this temperature. Nevertheless, the different proposed theories have different implications on phenomena such as the cold denaturation (and stop of activity) of proteins at low T , an important issue in cryopreservation, cryonics, cryostasis and cryobiology.

1.2. Interfacial water

One possible strategy to probe supercooled water at very low T is to consider water at an interface. Water adsorbed onto the surface of proteins or confined in nanopores freezes at much lower T than bulk water, giving access to a low temperature region where interfacial water is still liquid, while bulk water would not be [22]. In many cases of interest for practical purposes in biology, geology or industrial applications, water is hydrating a surface or is confined. As a consequence, fundamental research in physics and chemistry has been performed in recent years with experiments [21, 23–29, 22, 30], theories and simulations [31–34].

During the last years experiments on water in Vycor micropores [35], in nanopores of MCM-41 silica [36–38], of sol–gel silica glass [39], of NaA zeolites [40], or of double-wall carbon nanotubes [41] have contributed to the investigation of water dynamics in confinement. In particular, confinement in hydrophilic MCM-41 silica nanopores of 1.8 and 1.4 nm diameter allows to study water dynamics down to 200 K where quasielastic neutron scattering reveals a crossover at $T \approx 225 \text{ K}$ in the average translational relaxation time from a non-Arrhenius behavior at high T to an Arrhenius behavior at low T [42]. A similar crossover is also observed for the self-diffusion coefficient of water by nuclear magnetic resonance at $T \approx 223 \text{ K}$ [43]. By increasing from 400 bars to 1600 bars the external pressure applied on a sample of MCM-41 silica nanopores with 1.4 nm diameter at full hydration level of 0.5 g of H_2O per g of silica, it has been observed that the crossover occurs at lower T , reaching $T \approx 200 \text{ K}$ at $P = 1600 \pm 400 \text{ bars}$ and disappears at higher P [44].

Quasielastic neutron scattering experiments show the same crossover for the average translational relaxation time of at least three different systems: (i) water hydrating lysozyme, at hydration level $h = 0.3 \text{ g of H}_2\text{O per g of dry lysozyme}$, for

$T \approx 220$ K, a temperature below which the protein has a glassy dynamics [30], (ii) DNA hydration water, at hydration level corresponding to about 15 water molecules per base pairs, for $T \approx 222$ K, at which DNA displays the onset of anharmonic molecular motion [45], and (iii) RNA hydration water, at a similar hydration level, for $T \approx 220$ K, where both RNA and its hydration water exhibit a sharp change in slope for the mean-square displacements of the hydrogen atoms [46].

All these results can be interpreted as a consequence of a structural rearrangement of water molecules associated with a LDL–HDL critical point [44]. In fact, along the Widom line in the supercritical region of the LDL–HDL critical point, the changes in the hydrogen bond network are consistent with the dynamic behavior observed in the experiments, as we will discuss in the following sections.

This interpretation has been criticized [47] on the base of similar crossover observed for water confined in molecular sieves [48] or for water mixtures [49] and water solutions [50]. It has also been proposed a possible interpretation as a consequence of the dynamics of (Bjerrum-type) defects due to orientationally disordered water molecules that are hydrogen bonded to less than four other water molecules [51, 52].

^2H -NMR studies on hydrated proteins, at a comparable hydration level as in [44], show no evidence for the crossover at 220 K and indicate that water performs thermally activated and distorted tetrahedral jumps at $T < 200$ K, which may be related to a universal defect diffusion [28]. Also, dielectric spectroscopy studies of hydrated protein show a smooth temperature variations of conductivity at 220 K and ascribe the crossover observed in neutron scattering to a secondary relaxation that splits from the main structural relaxation [29, 53].

On the other hand, numerical simulations for bulk water show that, on crossing the Widom line emanating from a LDL–HDL critical point, the structural change in water is maximum, as emphasized by the maximum in specific heat, and the diffusion constant has a crossover [54]. This result is observed also in simulations of water hydrating lysozyme or DNA, where the macromolecules change their dynamics at the crossover temperature of the hydration water diffusivity, coinciding with the temperature of maximum change of water structure [55].

A crossover at about 223 K from high- T non-Arrhenius to low- T Arrhenius behavior, in agreement with the neutron scattering experiments, is observed also in simulation of water hydrating lysozyme powder for the translational correlation time and for the inverse of the self-diffusion constant [56]. The activation energy for the Arrhenius regime is found to be of about 0.15 eV, as in the neutron scattering experiments [56]. Also, simulations of water hydrating elastin-like and collagen-like peptides show this crossover, but with a weaker change in the slope and an Arrhenius activation energy of about 0.43 eV, consistent with dielectric spectroscopy and nuclear magnetic resonance studies [57, 28].

It is therefore difficult not only in the experiments, but also in the models to get a clear answer about the relevant dynamic mechanisms and their relation with the thermodynamics in water at interfaces. Moreover, the relation between confined

water and bulk water remains not fully understood. For this reason models that are tractable with a theoretical approach are particularly appealing in this context. With these models, in fact, simulations can be compared with analytic calculations to develop a consistent theory.

In the following we will present a coarse-grained model that reproduces the experimental dynamics and thermodynamics of water and has two relevant features: (i) it is tractable within theoretical approaches, and (ii) it can be equilibrated in simulations at very low T , where other models require an extremely larger computational time. After defining the model in section 2, we will summarize our recent results about the thermodynamics and the dynamics of this model. In section 3 we will recall bulk results, showing new data from extended simulations and their finite-size analysis to prove in a clear way the occurrence of a LDL–HDL first-order phase transition at low T and high P . Next, in section 3.1, we present new theoretical calculations and Monte Carlo simulations for the phase diagram and how it depends on a parameter that characterizes the cooperativity of the model. In section 4, we describe our on-going investigation about the effects of interfaces on the dynamics and thermodynamics of water. Finally, in section 5, we present some conclusions.

2. Cooperative cell model for a monolayer of water

We consider the case of water in $d = 2$ -dimensions. This case can be considered as an extreme confinement of one single layer of water between two repulsive (hydrophobic) walls when the distance between the walls is such to inhibit the crystal formation [58]. In fact, it has been shown that the relevant parameter to avoid the transition to a crystal phase is the distance between the confining wall and not the characteristics of the hydrophobic interaction with the wall [58].

Another case in which the study of a monolayer of water is relevant is when a substrate of protein powder is, on average, hydrated only by a single layer of water, and the proteins do not undergo any configurational transformation and/or large scale motion [59]. In these conditions, for a hydrophilic protein surface, we can assume that the effect of the water–protein interaction is to attract water on a surface that, by constraining the water molecule positions, inhibits its crystallization.

A very desirable feature of a model for a liquid is transferability. The parameters and effective interactions of a model are optimized to precisely reproduce static and dynamic properties of the liquid at one particular thermodynamic state point. The quality of the model is measured by the range of validity of its predictions in other state points. Unfortunately, there is no water model that is truly transferable, nor can reproduce all the properties of water [60]. Many routes have been explored to solve this issue. Molecular polarizability [61, 62] is one way to introduce effects not considered by standard pairwise additive potentials. However, polarizable models are computationally very expensive and provide only a partial solution [63]. An alternative way is to include many-body effects into the potential. In the following we define a model with an effective many-body interaction introduced through a cooperative hydrogen bond term.

2.1. Definition of the model with cooperative interaction

We consider N molecules in a volume V with periodic boundary conditions (p.b.c.) in $d = 2$ -dimensions, and the size of less than or about four molecules (and no p.b.c.) in the third dimension. We initially consider the case in which the molecules are distributed in a homogeneous way, with each molecule $i \in [1, N]$ occupying the same volume V/N larger than a hard-core volume $v_0 \approx 102 \text{ \AA}^3$ due to short-range electron clouds repulsion. We consider the case in which each molecule has coordination number four, consistent with the tendency of a water molecule to minimize its energy by forming four hydrogen bonds. By considering a layer thickness of about four molecules, we allow water to form a non-flat monolayer, whose projection on a plane form a square lattice, but that in $d = 3$ resembles a distorted tetrahedral structure with each molecule having a nearest neighbor on the same plane and three neighbors in two distinct planes.

The interaction Hamiltonian for water molecules is [64–66, 5]

$$\mathcal{H} = U_0(r) - J \sum_{\langle i, j \rangle} \delta_{\sigma_{ij}, \sigma_{ji}} - J_\sigma \sum_{(k, l)_i} \delta_{\sigma_{ik}, \sigma_{il}} \quad (1)$$

where $U_0(r)$ denotes the sum of all the isotropic interactions (e.g. van der Waals) between molecules at distance $r \equiv (V/N)^{1/d}$, represented by a Lennard-Jones potential with attractive energy ϵ plus a hard-core at distance $r_0 \equiv (v_0)^{1/d}$.

The second term (with $\delta_{a,b} = 1$ if $a = b$ and $\delta_{a,b} = 0$ otherwise, and $\langle i, j \rangle$ denoting that i and j are nearest neighbors) accounts for the directional contribution to the hydrogen bond energy with strength J , where $\sigma_{ij} = 1, \dots, q$ is a (Potts) variable representing the orientational state of the hydrogen (or the lone e^- pair) of molecule i facing the lone e^- pair (or the hydrogen, respectively) of the molecules j . For the sake of simplicity we do not distinguish between hydrogens and lone e^- pairs, associating to each molecule four equivalent bond indices σ_{ij} , one for each possible bonding ‘arm’. We choose the parameter q by selecting 30° as the maximum deviation from a linear bond, i.e. setting the O–H...O angle to less than 30° , as estimated from Debye–Waller factors [67, 68]. Hence, each molecular arm has $q \equiv 180^\circ/30^\circ = 6$ possible states: $q - 1$ are non-bonding and one, such that $\delta_{\sigma_{ij}, \sigma_{ji}} = 1$, is bonding. Every molecule has $q^4 = 6^4 \equiv 1296$ possible states. The variables σ_{ij} , therefore, do not represent orientations of the arms, but their bonding state. In this sense they are not related to each other by molecular rigidity. However, at variance with what hypothesized in [20], we consider that they are correlated through the third term of the Hamiltonian in equation (1), as explained in the following. The effect of choosing a different value for q has been analyzed in [5].

The third term (with $(k, l)_i$ indicating each of the six different pairs of the four bond indices of molecule i) accounts for the correlation among the arms of a molecule. It originates from the water many-body interaction, that is revealed by the experimental O–O–O correlation [25], locally driving the molecules toward an ordered (tetrahedral in the bulk) configuration with lower energy. This term introduces the hydrogen bond cooperativity in our model.

By defining the energy per hydrogen bond (between σ_{ij} and σ_{ji}) as the sum of the interactions in which two bonded molecules (i and j) are participating, we obtain $E_{\text{HB}} = \epsilon + J + mJ_\sigma/2$, where $m = 0, \dots, 6$ is the number of cooperative interactions in which that bond variables (σ_{ij} and σ_{ji}) are partaking. If we choose as parameters $\epsilon = 5.8 \text{ kJ mol}^{-1}$ (consistent with the value 5.5 kJ mol^{-1} of the estimate of the van der Waals attraction based on isoelectronic molecules at optimal separation [69]), $J = 2.9 \text{ kJ mol}^{-1}$ and $J_\sigma = 0.29 \text{ kJ mol}^{-1}$, the values of E_{HB} ranges between 8.70 kJ mol^{-1} and 9.6 kJ mol^{-1} depending on m . However, a definition of E_{HB} based on a cluster of 5 or 8 bonded molecules in $d = 3$ -dimensions increases this range up to 17 kJ mol^{-1} or 18 kJ mol^{-1} , respectively. Therefore, E_{HB} depends on the environment (the value of m and the number of molecules bonded in a cluster), as observed in computer simulation of the crystalline phases of ice [70], and has values within the range 6.3 kJ mol^{-1} [71]– 23.3 kJ mol^{-1} [72], proposed on the base of experiments.

Experiments show that formation of the hydrogen bonds leads to an open-locally tetrahedral structure that induces an increase of volume per molecule [73, 16]. This effect is incorporated in the model by considering that a full bonded molecule, i.e. a molecule with four hydrogen bonds, has a molecular volume larger than a non-bonded molecule by an amount

$$\Delta v \equiv 4v_{\text{HB}}, \quad (2)$$

where v_{HB} is the volume increase per H bond. Hence, if

$$N_{\text{HB}} \equiv \sum_{\langle i, j \rangle} n_i n_j \delta_{\sigma_{ij}, \sigma_{ji}} \quad (3)$$

is the total number of hydrogen bonds in the system, the hydrogen bond contribution to the total volume is

$$\Delta V \equiv N_{\text{HB}} v_{\text{HB}}. \quad (4)$$

We adopt $r_0 = 2.9 \text{ \AA}$ consistent with the expected value of the van der Waals radius [74], and $v_{\text{HB}} = 0.5v_0$, with $v_0 \equiv r_0^3$, corresponding to a maximum hydrogen bond distance of about 3.3 \AA , consistent with the range of a water molecule’s first coordination shell, 3.5 \AA , as determined from the oxygen–oxygen radial distribution function [75].

3. The phase diagram

The model is studied using both mean field (MF) analysis and Monte Carlo (MC) simulations. The MF approach has been describe in details in [5, 76]. It consists of expressing the molar Gibbs free energy in terms of an exact partition function for a portion of the system made of a treatable number of degrees of freedom. We, therefore, take into account local fluctuations at the scale of the considered portion of the system. We take into account the effect of all the rest of the system as a mean field acting on the border of this portion [5, 64–66, 76–82]. This method has many similarities with the Bethe Peierls and the cavity method [83].

MC simulations are performed at constant N , P , T , allowing the volume V_{MC} of the system to fluctuate

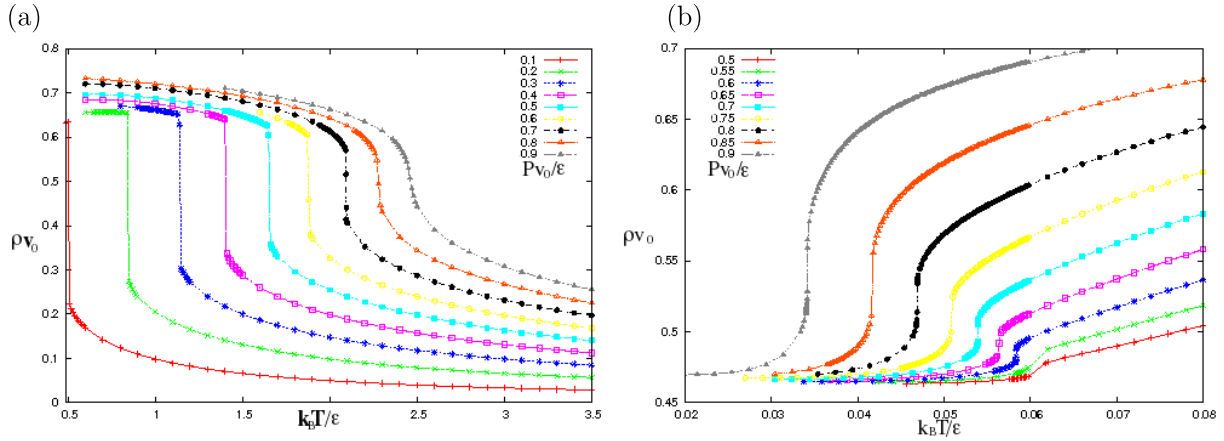


Figure 1. The density ρ (in units of $1/v_0$) as a function of the temperature T (in units of ϵ/k_B where k_B is the Boltzmann constant) for different values of pressure P (in units of ϵ/v_0) as calculated from MC simulation of a system with $N = 15\,625$ water molecules. The parameters of the model are $J/\epsilon = 0.5$, $J_\sigma/\epsilon = 0.05$ and $v_{HB}/v_0 = 0.5$. (a) At high T and for (from bottom to top) values of Pv_0/ϵ from 0.1 to 0.9, we observe for $Pv_0/\epsilon < 0.8$ a discontinuity in the density corresponding to the first-order gas–liquid phase transition. (b) At low T and for (from bottom to top) Pv_0/ϵ from 0.5 to 0.9, for $Pv_0/\epsilon > 0.55$ a discontinuity in ρ marks the first-order LDL–HDL phase transition.

as a stochastic variable. The average distance r between nearest neighbors molecules is then calculated as $r/r_0 \equiv (V_{MC}/v_0N)^{1/d}$. The total volume of the system is by definition

$$V \equiv V_{MC} + \Delta V, \quad (5)$$

where ΔV is the hydrogen bond volume contribution in equation (4). Note that ΔV is not included in the calculation of r to avoid MF-type long-range correlation of volume fluctuations in the MC simulations.

For the parameters choice $J/\epsilon = 0.5$, $J_\sigma/\epsilon = 0.05$ and $v_{HB}/v_0 = 0.5$, we find that the density ρ as a function of T at constant P displays a discontinuous change at high T and low P corresponding to the gas–liquid first-order phase transition ending in a critical point, where the discontinuity disappears, at about $P_C = (0.75 \pm 0.05)\epsilon/v_0$ and $T_C = (2.2 \pm 0.1)\epsilon/k_B$ (figure 1(a)). If we choose as model parameters $\epsilon = 2.5 \text{ kJ mol}^{-1}$ and $r_0 = 3.2 \text{ \AA}$, we get an estimate $P_C = (22.7 \pm 1.5) \text{ MPa}$ and $T_C = (661 \pm 30) \text{ K}$ consistent with the real water critical point at about 22.064 MPa and 647 K. By decreasing T , the density reaches a maximum, that in real water at atmospheric pressure occurs at 4°C. At lower T , in the supercooled state, and higher P we find another discontinuity in density, this time with a lower density at lower T (figure 1(b)). The system at these supercooled T displays a first-order phase transition from HDL to LDL, as hypothesized in the LLCP scenario (figure 2).

3.1. Effect of hydrogen bond cooperativity on the behavior of water

The experiments for confined water have boosted the debate over the supercooled phase diagram of water, motivating the proposal of the CPF scenario hypothesized by Angell [21], as described above. This new scenario leads to questions such as

- (i) How to understand the new Angell hypothesis?
- (ii) How to connect it to the other three existing hypotheses?

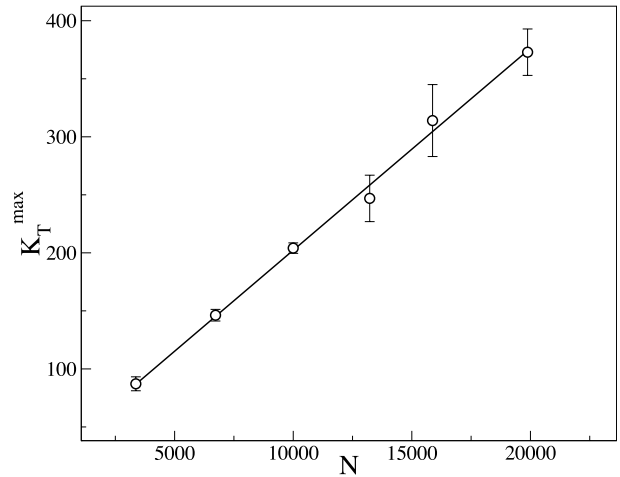


Figure 2. The finite-size behavior of the maximum of compressibility K_T^{\max} as a function of the number of water molecules N for pressure $P = 0.8\epsilon/v_0$ at low T shows a linear increase as expected at a first-order phase transition.

A recent work by Stokely *et al* [84] succeeds in answering both questions (i) and (ii). Specifically, it is shown that all four existing hypotheses are cases of the cooperative water model. Thus no matter which hypothesis may be correct (if any is correct), it is possible that the underlying mechanism is basically the same—the thermodynamic properties of water can be accounted for by considering two main contributions to the hydrogen bond interaction: (a) the directional (or covalent) contribution (parametrized by J in the model) and (b) the many-body (or cooperative) contribution (parametrized by J_σ in the model).

By MF calculations and MC simulations, Stokely *et al* [84] demonstrate that the balance between contributions (a) and (b) determines which of the four hypotheses presented in section 1.1 best describes experimental facts. Since the characteristic energy associated with these two contributions

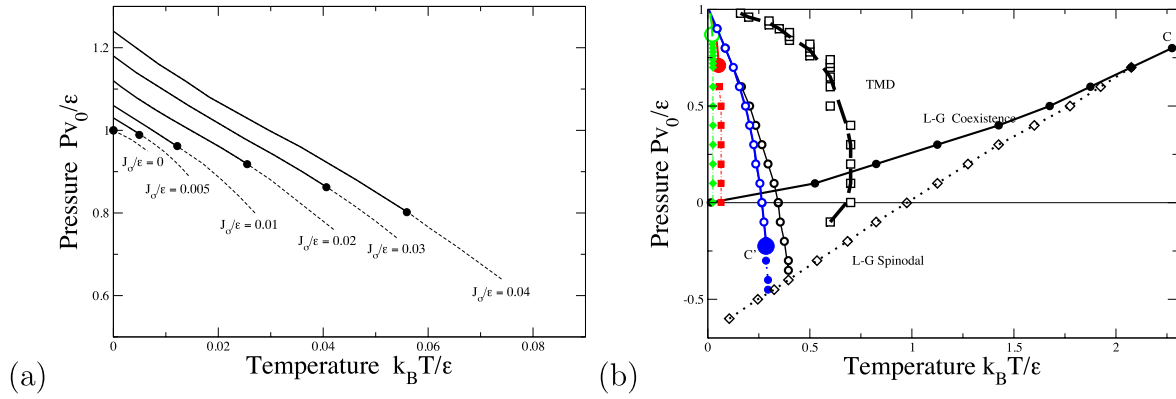


Figure 3. The pressure P versus temperature T phase diagram of the cooperative water model for different values of J_σ/ϵ . (a) Mean field results showing the low T phase diagram with the LDL–HDL phase transition lines (solid lines, where K_T is discontinuous) and Widom lines (dashed lines, where K_T has a finite maximum) for varying J_σ/ϵ from (rightmost) 0.04, 0.03, 0.02, 0.01, 0.005 and 0 (leftmost). For each value of J_σ/ϵ solid circles indicate the LDL–HDL critical point C' where the response function (such as K_T) diverge. Hashed circle indicates the state point at $T = 0$ where K_T diverges when $J_\sigma/\epsilon = 0$. (b) The MC phase diagram for varying J_σ/ϵ for $N = 10^4$ water molecules. At high T the system displays a liquid–gas first-order phase transition line (continuous line with full circles) ending in a liquid–gas critical point C (full circle), from which departs the liquid-to-gas spinodal line (dashed line with open diamonds). At lower T , the retracing line with open squares marks the temperatures of maximum density (TMD) along isobars. All these loci do not change in an appreciable way by changing the value of J_σ/ϵ . The phase diagram at lower T , instead, show a strong dependence from J_σ/ϵ . For $J_\sigma/\epsilon = 0.5$, we find for any P above the spinodal line a first-order phase transition line between a HDL (at high P) and a LDL (at low P) phase (continuous line with open circles). This is the CPF scenario [21]. The analysis of the HDL-to-LDL (not shown) reveals that the limit of stability of the HDL phase retraces to positive P as in the SF scenario [17]. For $J_\sigma/\epsilon = 0.3$ we observe that the HDL–LDL phase transition ends in a critical point C' (continuous line with open circles ending in a full large circle) at negative P , as in the LLC scenario suggested in [19]. From C' a Widom line (dashed line with full circles) departs. For $J_\sigma/\epsilon = 0.05$, C' occurs at positive P , as hypothesized in [18] and the Widom line (dashed line with full squares) extends to lower P . For $J_\sigma/\epsilon = 0.02$, C' approaches the $T = 0$ axis, as well as the Widom line (dashed line with full diamonds), going toward the limit of the SF scenario [20].

can be estimated, the work allows to begin to validate or contradict each hypothesis on an experimental basis.

Specifically, by fixing the parameters $J/\epsilon = 0.5$ and $v_{HB}/v_0 = 0.5$, and varying the parameter J_σ/ϵ , it is possible to observe that the cooperative model reproduces all four scenarios of section 1.1. The overall picture that emerges is one in which the amount of cooperativity among H bonds (J_σ/ϵ), in relation to the H bond directional strength (J/ϵ), governs the location of a LLC, hence which scenario is realized. For zero cooperativity, the temperature T_C where K_T^{\max} and α_P^{\max} diverge is at zero temperature, and no liquid–liquid transition exists for $T > 0$ —the SF scenario. For very large cooperativity, C' lies outside the region of stable liquid states, and a liquid–liquid transition extends to the entire (supercooled and superheated) liquid phase—the CPF/SL scenario. For intermediate values of H bond cooperativity, T_C varies in a smooth way between these two extremes—the LLC scenario. Due to the anticorrelation between the volume and entropy associated to the H bonds, the larger T_C , the smaller P_C , eventually with $P_C < 0$ for larger cooperativity. These cases are summarized in figure 3.

4. Water at interfaces

To elucidate the relation between the protein dynamic crossover at about 220 K and the dynamic crossover observed for the average translational correlation time in the first layer of protein hydration water [30, 44–46], we perform MF calculations and MC simulations of the cooperative model of

water of section 2.1. Since we are interested in cases at low humidity, we consider the case of a water monolayer hydrating an immobile surface of globular protein that, forcing the water molecules out of place with respect to crystal configurations, inhibits the crystallization. We focus on the hydrogen bonds dynamics, regardless if the hydrogen bonds are formed with the protein or among water molecules. For the sake of simplicity, here we do not include in our description that protein–water hydrogen bonds could have a different strength from water–water hydrogen bonds, leaving this possibility for future extensions of the model.

4.1. The hydrogen bond dynamics for hydrated proteins

Following the work of Kumar *et al* [79–81], Mazza *et al* [59] study the orientational correlation time τ associated with the hydrogen bond dynamics of the model described in section 2.1. They confirm the occurrence of a dynamic crossover at a temperature of about $k_B T/\epsilon \approx 0.32$ corresponding to the T of maximum variation of the number of hydrogen bonds, that in turn corresponds to the Widom line. They also confirm that the crossover is from a non-Arrhenius behavior at high T to another non-Arrhenius behavior [82], that closely resembles an Arrhenius behavior around the crossover.

These results are consistent with those from simulations of other models for hydrated proteins where a crossover in the translational dynamics is observed [55]. The difference here is that (i) the crossover is for the dynamics of the hydrogen bonds, (ii) in the cooperative water model the crossover can be calculated from MF and an exact relation can be found between

the crossover and the Widom line, and (iii) the model can test different hypotheses. In particular, Kumar *et al* have shown that the crossover at $k_B T/\epsilon \approx 0.32$ is independent of whether water at very low temperature is characterized by a LLCP or is SF. In fact, the crossover is a consequence of the sharp change in the average number of hydrogen bonds at the temperature of the specific heat maximum, that occurs in both scenarios. Kumar *et al* were able also to make predictions about the P -dependence of quantities characterizing the crossover at $k_B T/\epsilon \approx 0.32$: (i) the timescale of the crossover, showing that it is independent of P (isochronic crossover); (ii) the activation energy of the apparent Arrhenius behavior at low T and (iii) the crossover temperature, showing that both (ii) and (iii) decrease linearly upon increasing P [80]. These predictions have been confirmed by Chu *et al* [85, 82] in a study on the dynamics of a hydrated protein under moderately high pressures at low temperatures using the quasielastic neutron scattering method. They relate these predictions (i)–(iii) to the mechanical response of the protein to an external force, that is the average elastic constant calculated from the mean-square displacement of the protein atoms. In particular, the degree of ‘softness’ of the protein, related to the enzymatic activity, is preserved at lower T if the pressure is increased [85]. However, a criterion proposed in [80] for discriminating which scenario better describe water on the basis of the crossover at $k_B T/\epsilon \approx 0.32$, cannot be tested in the experiments since the predicted difference between the two scenarios (of the order of 1%) is within the error bars of the measurements [82].

The answer to the puzzle of which of the scenarios better describe water might be related to the very recent experimental discovery of another crossover for the hydrogen bond τ to an Arrhenius behavior at very low T , of the order of 180 K at hydration $h = 0.3$ g H₂O/g of dry protein. This crossover has been observed by Mazza *et al* at $k_B T/\epsilon \approx 0.07$ [59], in relation to an ordering process of the hydrogen bonds leading to the HDL–LDL critical point. The study has been possible thanks to the use of a highly efficient cluster MC dynamics [86, 87]. This very low T crossover would reduce even more the T at which the proteins preserve their ‘softness’, essential for their correct functionality.

4.2. Water monolayer in hydrophobic confinement

By considering partially hydrated hydrophobic plates at a distance such to inhibit the crystallization of water at low T , Franzese and de los Santos [88] have show that water has a glassy behavior [89] for both the translational and rotational degrees of freedom when cooled down to a low P . This result is consistent with simulations of TIP4P water forming a quasi-2d amorphous when confined in a hydrophobic slit pore with wall-to-wall separation just enough to accommodate two molecular layers [90].

At higher P the hydrogen bond network builds up in a less gradual way, allowing the system to equilibrate the rotational degrees of freedom also at very low T , but not the translational degrees of freedom. This effect is emphasized by the appearance of many dehydrated regions [88], as also observed in water confined between two protein-like

hydrophobic flattened surfaces at distances ranging from 0.4 to 1.6 nm [33].

When P is close to the LLCP value, the cooperativity of the hydrogen bond network induces a strong non-exponential behavior [91] for the hydrogen bond correlation function. However, both rotational and translational degrees of freedom equilibrate within the simulation time. At higher P the rotational correlation function recovers the exponential behavior and the diffusion of the system allows the formation of a large dry cavity, while the rest of the surface is well hydrated. It is interesting to observe that the cooperative model allows to calculate, in the MF approximation, the diffusion constant at any T and P [92].

The hydrophobic confinement has effects also on water thermodynamics. It shifts the HDL–LDL phase transition to lower temperature and lower pressure, as compared to bulk water, when the confinement is between plates [93, 94]. Moreover, it shifts both the line of maximum density and the liquid-to-gas spinodal toward higher pressures and lower temperatures with respect to bulk when the confinement is in a hydrophobic disordered matrix of soft spheres [34]. This result is confirmed also in the analysis performed by using the cooperative water model in confinement between hydrophobic hard spheres [95]. However, the effect of the matrix on the HDL–LDL critical point is less clear and is presently under investigation.

5. Conclusions

The effect of confinement is of great interest to biology, chemistry, and engineering, yet the recent experimental and simulations results are object of an intense debate. A better understanding of the physico-chemical properties of liquid water at interfaces is important to provide accurate predictions of the behavior of biological molecules [96], including the folding–unfolding transitions seen in proteins [97–99], and the dynamical behavior of DNA [45]. However, it is still unclear whether such behaviors are inherent in the structure of such molecules, or an effect of water in which they are always found, or due to the interactions between the two.

To get insight into this subject the formulation of a model that allows the development of a theory could be useful to find functional relations connecting different observables. The advantage of this approach is to have two independent ways of approaching the problem, one theoretical and the other numerical.

We have presented here several recent results obtained with a cooperative water model suitable for studies with mean field theories and with N , P , T simulations with thousands of molecules. The model has been studied in the context of water monolayers on hydrated proteins, between hydrophobic surfaces or in a hydrophobic matrix.

Some of the conclusions reached with this model are the following:

- The different scenarios proposed to interpret the low- T behavior of water are instances of the same mechanism, with different values of the directional (covalent) strength and the cooperative (many-body) interaction of the

hydrogen bonds. The parameters that can be estimated from the experiments suggest that the scenario with the LLCP is the most plausible for water.

- Previous experiments showing one dynamic crossover in the water monolayer hydrating proteins, RNA and DNA are consistent with (at least) two scenarios.
- The possibility of a second dynamic crossover detectable at lower T and lower hydration level would be consistent only with the LLCP scenario, because its origin would be related to the ordering of the hydrogen bond network.
- A consequence of the occurrence of a LLCP should be detectable when the translational and rotational dynamics of water are studied for a monolayer in a hydrophobic confinement. In particular, the rotational dynamics should appear with the strongest non-exponential behavior in the vicinity of the LLCP, as an effect of the cooperativity. Moreover, the slow increase of the number of hydrogen bonds at low T and low P is the cause of the formation of an amorphous glassy state when the confinement is such to inhibit the crystallization of water. Under this conditions, the dehydration of hydrophobic surfaces is characterized by the appearance of heterogeneities and cavitation.
- The hydrophobic confinement affects the thermodynamics of water by lowering the T and increasing the P of the liquid–gas phase transition and of the TMD line. It also affects the LDL–HDL phase transition in a way that is possibly more complex.

All these results are potentially relevant in problems such as protein denaturation or protein aggregation. Works are in progress to underpin and build up a theory of water at interfaces that could help us to acquire a better understanding of these subjects.

Acknowledgments

This paper is a contribution that concerns recent progress in the field of computer simulations of water discussed at the CECAM workshop ‘Modeling and Simulation of Water at Interfaces from Ambient to Supercooled Conditions’ supported by ESF-Simbioma and CECAM.

This work was partially supported by the Spanish Ministerio de Ciencia e Innovación Grants Nos FIS2005-00791 and FIS2009-10210 (co-financed FEDER), Junta de Andalucía Contract No. FQM 357.

References

- [1] Debenedetti P G and Stanley H E 2003 *Phys. Today* **56** 40–6
- [2] Angell C A and Tucker J C 1973 *Science* **181** 342–4
- [3] Speedy R J and Angell C A 1976 *J. Chem. Phys.* **65** 851–8
- [4] Hare D E and Sorensen C M 1986 *J. Chem. Phys.* **84** 5085–9
- [5] Franzese G and Stanley H E 2007 *J. Phys.: Condens. Matter* **19** 205126
- [6] Debenedetti P G 1996 *Metastable Liquids. Concepts and Principles* (Princeton, NJ: Princeton University Press)
- [7] Salzmann C G, Radaelli P G, Mayer E and Finney J L 2009 *Phys. Rev. Lett.* **103** 105701
- [8] Bruggeller P and Mayer E 1980 *Nature* **288** 569–71
- [9] Jenniskens P and Blake D 1994 *Science* **265** 753–6
- [10] Mishima O, Calvert L and Whalley E 1985 *Nature* **314** 76–8
- [11] Strazzulla G, Baratta G A, Leto G and Foti G 1992 *Europhys. Lett.* **18**
- [12] Loerting T and Giovambattista N 2006 *J. Phys.: Condens. Matter* **18** R919–77
- [13] Burton E F and Oliver W F 1935 *Proc. R. Soc. A* **153** 166–72
- [14] Mishima O, Calvert L and Whalley E 1984 *Nature* **310** 393–5
- [15] Loerting T, Salzmann C, Kohl I, Mayer E and Hallbrucker A 2001 *Phys. Chem. Chem. Phys.* **3** 5355–7
- [16] Soper A and Ricci M 2000 *Phys. Rev. Lett.* **84** 2881–4
- [17] Speedy R J 1982 *J. Phys. Chem.* **86** 3002–5
- [18] Poole P, Sciortino F, Essmann U and Stanley H 1992 *Nature* **360** 324–8
- [19] Tanaka H 1996 *Nature* **380** 328
- [20] Sastry S, Debenedetti P G, Sciortino F and Stanley H E 1996 *Phys. Rev. E* **53** 6144–54
- [21] Angell C A 2008 *Science* **319** 582–7
- [22] Mallamace F, Branca C, Broccio M, Corsaro C, Mou C Y and Chen S H 2007 *Proc. Natl Acad. Sci. USA* **104** 18387–91
- [23] Granick S and Bae S C 2008 *Science* **322** 1477–8
- [24] Faraone A, Liu K H, Mou C Y, Zhang Y and Chen S H 2009 *J. Chem. Phys.* **130** 134512
- [25] Ricci M A, Bruni F and Giuliani A 2009 *Faraday Discuss.* **141** 347–58
- [26] Soper A K 2008 *Mol. Phys.* **106** 2053–76
- [27] Bellissent-Funel M C 2008 *J. Phys.: Condens. Matter* **20** 244120
- [28] Vogel M 2008 *Phys. Rev. Lett.* **101** 225701
- [29] Pawlus S, Khodadadi S and Sokolov A P 2008 *Phys. Rev. Lett.* **100** 108103
- [30] Chen S H, Liu L, Fratini E, Baglioni P, Faraone A and Mamontov E 2006 *Proc. Natl Acad. Sci. USA* **103** 9012–6
- [31] Chandler D 2005 *Nature* **437** 640–7
- [32] Dill K A, Truskett T M, Vlachy V and Hribar-Lee B 2005 *Annu. Rev. Biophys. Biomol. Struct.* **34** 173–99
- [33] Giovambattista N, Lopez C F, Rosky P J and Debenedetti P G 2008 *Proc. Natl Acad. Sci. USA* **105** 2274–9
- [34] Gallo P and Rovere M 2007 *Phys. Rev. E* **76** 061202–7
- [35] Bellissent-Funel M C, Chen S H and Zanotti J M 1995 *Phys. Rev. E* **51** 4558–69
- [36] Takahara S, Nakano M, Kittaka S, Kuroda Y, Mori T, Hamano H and Yamaguchi T 1999 *J. Phys. Chem. B* **103** 5814–9
- [37] Faraone A, Liu L, Mou C Y, Shih P C, Copley J R D and Chen S H 2003 *J. Chem. Phys.* **119** 3963–71
- [38] Chen S H, Mallamace F, Mou C Y, Broccio M, Corsaro C, Faraone A and Liu L 2006 *Proc. Natl Acad. Sci.* **103** 12974–8
- [39] Crupi V, Majolino D, Migliardo P and Venuti V 2002 *J. Phys. Chem. B* **106** 10884–94
- [40] Crupi V, Majolino D, Migliardo P, Venuti V, Wanderlingh U, Mizota T and Telling M 2004 *J. Phys. Chem. B* **108** 4314–23
- [41] Chu X Q, Kolesnikov A I, Moravsky A P, Garcia-Sakai V and Chen S H 2007 *Phys. Rev. E* **76** 021505–6
- [42] Faraone A, Liu L, Mou C Y, Yen C W and Chen S H 2004 *J. Chem. Phys.* **121** 10843–6
- [43] Mallamace F, Broccio M, Corsaro C, Faraone A, Wanderlingh U, Liu L, Mou C Y and Chen S H 2006 *J. Chem. Phys.* **124** 161102
- [44] Liu L, Chen S H, Faraone A, Yen C W and Mou C Y 2005 *Phys. Rev. Lett.* **95** 117802
- [45] Chen S H, Liu L, Chu X, Zhang Y, Fratini E, Baglioni P, Faraone A and Mamontov E 2006 *J. Chem. Phys.* **125** 171103
- [46] Chu X Q, Fratini E, Baglioni P, Faraone A and Chen S H 2008 *Phys. Rev. E* **77** 011908
- [47] Cerveny S, Colmenero J and Alegría A 2006 *Phys. Rev. Lett.* **97** 189802
- [48] Jansson H and Swenson J 2003 *Eur. Phys. J. E* **12** 51–4
- [49] Sudo S, Tsubotani S, Shimomura M, Shinyashiki N and Yagihara S 2004 *J. Chem. Phys.* **121** 7332–40

- [50] Cervený S, Schwartz G A, Alegría A, Bergman R and Swenson J 2006 *J. Chem. Phys.* **124** 194501
- [51] Swenson J 2006 *Phys. Rev. Lett.* **97** 189801
- [52] Swenson J, Jansson H and Bergman R 2008 *Aspects of Physical Biology: Biological Water, Protein Solutions, Transport and Replication (Lecture Notes in Physics vol 752)* ed G Franzese and M Rubi, pp 23–42
- [53] Khodadadi S, Pawlus S, Roh J H, Sakai V G, Mamontov E and Sokolov A P 2008 *J. Chem. Phys.* **128** 195106
- [54] Xu L, Kumar P, Buldyrev S V, Chen S H, Poole P H, Sciortino F and Stanley H E 2005 *Proc. Natl Acad. Sci. USA* **102** 16558–62
- [55] Kumar P, Yan Z, Xu L, Mazza M G, Buldyrev S V, Chen S H, Sastry S and Stanley H E 2006 *Phys. Rev. Lett.* **97** 177802
- [56] Lagi M, Chu X, Kim C, Mallamace F, Baglioni P and Chen S H 2008 *J. Phys. Chem. B* **112** 1571–5
- [57] Cervený S, Schwartz G A, Bergman R and Swenson J 2004 *Phys. Rev. Lett.* **93** 245702
- [58] Kumar P, Starr F W, Buldyrev S V and Stanley H E 2007 *Phys. Rev. E* **75** 011202
- [59] Mazza M G, Stokely K, Pagnotta S E, Bruni F, Stanley H E and Franzese G 2009 Two dynamic crossovers in protein hydration water, submitted
See also Mazza M G, Stokely K, Pagnotta S E, Bruni F, Stanley H E and Franzese G 2009 arXiv:0907.1810
- [60] Guillot B 2002 *J. Mol. Liq.* **101** 219–60
- [61] Lamoureux G, Alexander D, MacKerell J and Roux B 2003 *J. Chem. Phys.* **119** 5185–97
- [62] Mankoo P K and Keyes T 2008 *J. Chem. Phys.* **129** 034504
- [63] Piquemal J P, Chelli R, Procacci P and Gresh N 2007 *J. Phys. Chem. A* **111** 8170–6
- [64] Franzese G and Stanley H E 2002 *J. Phys.: Condens. Matter* **14** 2201–9
- [65] Franzese G and Stanley H E 2002 *Physica* **314** 508–13
- [66] Franzese G, Marques M I and Stanley H E 2003 *Phys. Rev. E* **67** 011103
- [67] Teixeira J and Bellissent-Funel M C 1990 *J. Phys.: Condens. Matter* **2** SA105–8
- [68] Luzar A and Chandler D 1996 *Phys. Rev. Lett.* **76** 928–31
- [69] Henry M 2002 *ChemPhysChem* **3** 561–9
- [70] Baranyai A, Bartók A and Chialvo A A 2005 *J. Chem. Phys.* **123** 054502
- [71] Smith J D, Cappa C D, Wilson K R, Messer B M, Cohen R C and Saykally R J 2004 *Science* **306** 851–3
- [72] Suresh S J and Naik V M 2000 *J. Chem. Phys.* **113** 9727–32
- [73] Debenedetti P G 2003 *J. Phys.: Condens. Matter* **15** R1669–726
- [74] Narten A, Danford M and Levy H 1967 *Discuss. Faraday Soc.* **97**
- [75] Soper A K and Phillips M G 1986 *Chem. Phys.* **107** 47–60
- [76] Stokely K, Mazza M G, Stanley H E and Franzese G 2010 *Metastable Systems under Pressure (NATO Science for Peace and Security Series A: Chemistry and Biology)* (Berlin: Springer) chapter (Metastable Water under Pressure) pp 197–216
- [77] Franzese G, Yamada M and Stanley H E 2000 *AIP Conf. Proc.* **519** pp 281–7
- [78] Franzese G and Stanley H E 2005 *Sci. Culture Ser.: Phys.* **26** 210–4
- [79] Kumar P, Franzese G and Stanley H E 2008 *J. Phys.: Condens. Matter* **20** 244114
- [80] Kumar P, Franzese G and Stanley H E 2008 *Phys. Rev. Lett.* **100** 105701
- [81] Kumar P, Franzese G, Buldyrev S V and Stanley H E 2008 *Aspects of Phys. Biology* **3–22**
- [82] Franzese G, Stokely K, Chu X Q, Kumar P, Mazza M G, Chen S H and Stanley H E 2008 *J. Phys.: Condens. Matter* **20** 494210
- [83] Mézard M and Parisi G 2001 *Eur. Phys. J. B* **20** 217–33
- [84] Stokely K, Mazza M G, Stanley H E and Franzese G 2010 *Proc. Natl Acad. Sci. USA* **107** 1301–6
- [85] Chu X Q, Faraone A, Kim C, Fratini E, Baglioni P, Leao J B and Chen S H 2009 *J. Phys. Chem. B* **113** 5001–6
- [86] Mazza M G, Stokely K, Strelakova E G, Stanley H E and Franzese G 2009 *Comput. Phys. Commun.* **180** 497–502
- [87] Cataudella V, Franzese G, Nicodemi M, Scala A and Coniglio A 1996 *Phys. Rev. E* **54** 175–89
- [88] Franzese G and de los Santos F 2009 *J. Phys.: Condens. Matter* **21** 504107
- [89] Kumar P, Franzese G, Buldyrev S V and Stanley H E 2006 *Phys. Rev. E* **73** 041505
- [90] Koga K, Tanaka H and Zeng X C 2000 *Nature* **564–7**
- [91] Franzese G and Coniglio A 1999 *Phys. Rev. E* **59** 6409–12
- [92] de los Santos F and Franzese G 2009 *Modeling and Simulation of New Materials: Proc. Modeling and Simulation of New Materials: Tenth Granada Lectures; AIP Conf. Proc.* **1091** 185–197
- [93] Truskett T M, Debenedetti P G and Torquato S 2001 *J. Chem. Phys.* **114** 2401–18
- [94] Kumar P, Buldyrev S V, Starr F W, Giovambattista N and Stanley H E 2005 *Phys. Rev. E* **72** 051503
- [95] Strelakova E G, Mazza M G, Stanley H E and Franzese G, in preparation
- [96] Ball P 2008 *Chem. Rev.* **108** 74–108
- [97] De Los Rios P and Caldarelli G 2000 *Phys. Rev. E* **62** 8449–52
- [98] Levy Y and Onuchic J N 2006 *Annu. Rev. Biophys. Biomol. Struct.* **35** 389–415
- [99] Dias C L, Ala-Nissila T, Karttunen M, Vattulainen I and Grant M 2008 *Phys. Rev. Lett.* **100** 118101